Cell Aggregation Culture Induces Functional Differentiation of Induced Hepatocyte-like Cells through Activation of Hippo Signaling
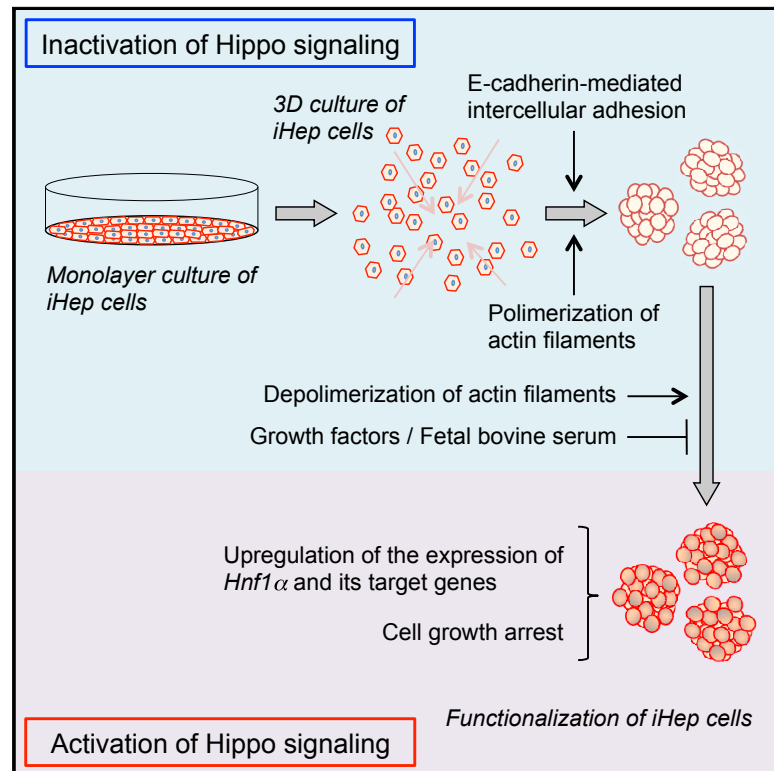
山本, 純平

Cell Aggregation Culture Induces Functional Differentiation of Induced Hepatocyte-like Cells through Activation of Hippo Signaling

Graphical Abstract

Authors

Junpei Yamamoto, Miyako Udono, Shizuka Miura, Sayaka Sekiya, Atsushi Suzuki

Correspondence

suzukicks@bioreg.kyushu-u.ac.jp

In Brief

Yamamoto et al. show that cell-aggregate formation induces functional differentiation of hepatocyte-like cells, designated iHep cells, which are directly induced from mouse fibroblasts. Hepatic maturation of iHep cells is regulated by activation of Hippo signaling that leads to upregulation of $Hnf1\alpha$ expression for induction of liver-enriched gene expression.

Highlights

- Cell aggregation culture induces growth arrest and hepatic maturation of iHep cells

- iHep cell aggregates efficiently and functionally reconstitute injured liver tissues

- Activation of Hippo signaling is essential for hepatic maturation of iHep cells

- $Hnf1\alpha$ expression upregulated in iHep cell aggregates is required for their maturation

Cell Aggregation Culture Induces Functional Differentiation of Induced Hepatocyte-like Cells through Activation of Hippo Signaling

Junpei Yamamoto,[1] Miyako Udono,[1] Shizuka Miura,[1] Sayaka Sekiya,[1] and Atsushi Suzuki[1,2,*]
[1]Division of Organogenesis and Regeneration, Medical Institute of Bioregulation, Kyushu University, Fukuoka 812-8582, Japan
[2]Lead Contact
*Correspondence: suzukicks@bioreg.kyushu-u.ac.jp
https://doi.org/10.1016/j.celrep.2018.09.010

SUMMARY

Recent progress in direct lineage reprogramming has enabled the generation of induced hepatocyte-like (iHep) cells and revealed their potential as an alternative to hepatocytes for medical applications. However, the hepatic functions of iHep cells are insufficient compared with those of primary hepatocytes. Here, we show that cell-aggregate formation can rapidly induce growth arrest and hepatic maturation of iHep cells through activation of Hippo signaling. During formation of iHep cell aggregates, Yap inactivation is induced by actin reorganization and intercellular adhesion, leading to upregulation of $Hnf1\alpha$ expression in the absence of the Yap/Tead/Chd4 transcriptional repressor unit. $Hnf1\alpha$ then acts as a central transcription factor that regulates liver-enriched gene expression in iHep cell aggregates and induces functional differentiation of iHep cells. Moreover, iHep cell aggregates efficiently reconstitute injured liver tissues and support hepatic function after transplantation. Thus, iHep cell aggregates may provide insights into basic research and potential therapies for liver diseases.
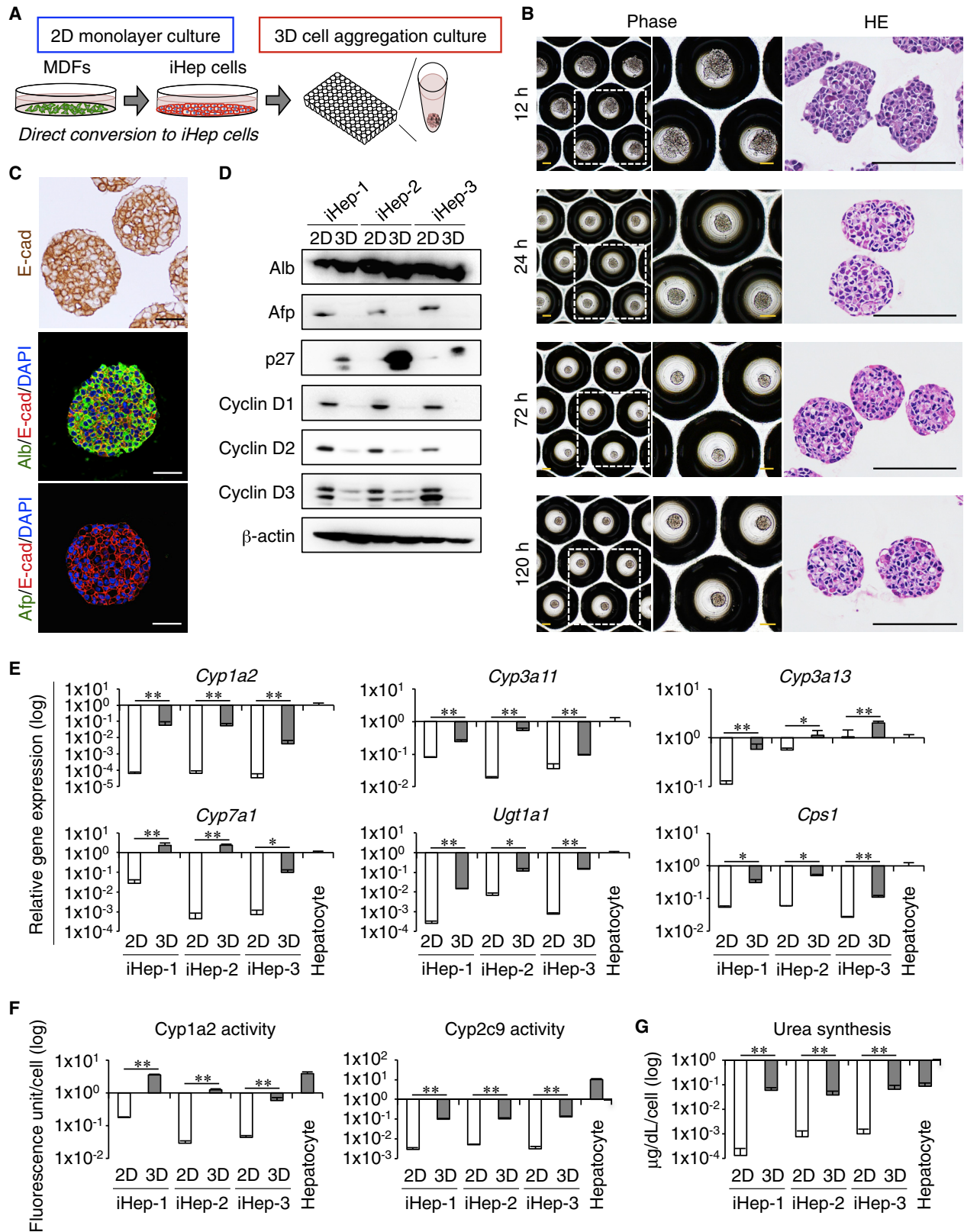
INTRODUCTION

Hepatocytes comprise 70%–80% of the liver and have specific functions in xenobiotic detoxification, lipid metabolism, glucose metabolism, and urea synthesis to maintain homeostasis (Miyajima et al., 2014; Si-Tayeb et al., 2010a). Thus, *in vitro* analyses of hepatocyte-specific properties are important for biomedical studies and drug development. However, because it is difficult to expand and maintain differentiated hepatocytes in culture (Desai et al., 2017; Guo et al., 2017; Khetani and Bhatia, 2008), alternative cell sources for hepatocytes are desirable for analyses of hepatic functions *in vitro*. As an alternative to hepatocytes, hepatocyte-like cells can be induced from embryonic stem cells (ESCs) and induced pluripotent stem cells (iPSCs) (Sancho-Bru et al., 2011; Si-Tayeb et al., 2010b). Furthermore, an approach involving direct reprogramming technology has enabled the generation of another alternative

cell source for hepatocytes, termed induced hepatocyte-like (iHep) cells, that can be induced from skin-derived fibroblasts by forced expression of defined transcription factors (Du et al., 2014; Huang et al., 2011, 2014; Sekiya and Suzuki, 2011). In our previous study, we found that a combination of hepatocyte nuclear factor 4α (Hnf 4α) and forkhead box a1 (Foxa1), Foxa2, or Foxa3 is sufficient for induction of iHep cells from mouse fibroblasts (Sekiya and Suzuki, 2011). iHep cells exhibit various hepatocyte-specific features and cell proliferation ability in monolayer culture and reconstitute liver tissues after transplantation into the livers of fumarylacetoacetate hydrolase (*Fah*)-deficient (*Fah*$^{-/-}$) mice as a mouse model of hereditary tyrosinemia type I (Overturf et al., 1996). Thus, iHep cells could potentially be used as an alternative to hepatocytes for the study and treatment of liver diseases. However, the levels of hepatic functions in iHep cells remain insufficient compared with those in primary hepatocytes in culture, and some cells in iHep cell cultures express the immature hepatic marker α-fetoprotein (Afp) (Huang et al., 2011; Sekiya and Suzuki, 2011). For these reasons, further differentiation of iHep cells should be induced before they can be used in medical applications. To resolve this issue, previous studies have suggested that iHep cells can acquire the properties of functionally mature hepatocytes by reconstituting hepatic tissues after transplantation (Huang et al., 2011; Sekiya and Suzuki, 2011). Thus, it is hypothesized that the formation of tissue-like structures in culture can induce functional differentiation of iHep cells.

Hepatic tissue-like structures formed by aggregation of primary hepatocytes in culture can prevent dedifferentiation of hepatocytes through upregulated expression of $Hnf4\alpha$ expression and suppressed expression of mesenchymal lineage markers *Vimentin* and *Snai1* (Chang and Hughes-Fulford, 2014). Cell-aggregate formation can also facilitate differentiation of ESCs into hepatocyte-like cells through increased expression of nuclear receptors, such as aryl hydrocarbon receptor (Ahr), constitutively active receptor (Car), and peroxisome proliferator activated receptor α (Pparα) (Takayama et al., 2013). Moreover, iPSC-derived hepatocyte-like cells can acquire hepatocyte-specific functions by forming cell aggregates, in which maintenance of cell-cell interactions among hepatocyte-like cells is important (Gieseck et al., 2014; Ogawa et al., 2013). Thus, it is suggested that iHep cells can become functionally close to hepatocytes by forming cell aggregates in culture.

A 2D monolayer culture / 3D cell aggregation culture

MDFs → iHep cells

Direct conversion to iHep cells

B Phase / HE (12 h, 24 h, 72 h, 120 h)

C E-cad / Alb/E-cad/DAPI / Afp/E-cad/DAPI

D iHep-1, iHep-2, iHep-3 (2D 3D): Alb, Afp, p27, Cyclin D1, Cyclin D2, Cyclin D3, β-actin

E Relative gene expression (log): *Cyp1a2*, *Cyp3a11*, *Cyp3a13*, *Cyp7a1*, *Ugt1a1*, *Cps1* (2D 3D iHep-1, iHep-2, iHep-3, Hepatocyte)

F Fluorescence unit/cell (log): Cyp1a2 activity, Cyp2c9 activity (2D 3D iHep-1, iHep-2, iHep-3, Hepatocyte)

G Urea synthesis — μg/dL/cell (log) (2D 3D iHep-1, iHep-2, iHep-3, Hepatocyte)

(legend on next page)

The present study demonstrates that cell-aggregate formation can rapidly induce growth arrest of iHep cells and their functional differentiation to hepatocytes in culture. Moreover, transplantation of iHep cell aggregates into the livers of $Fah^{-/-}$ mice significantly increased the lifespan of the recipient mice. Mechanistically, hepatic functionalization of iHep cells in cell aggregation cultures was regulated by activation of Hippo signaling, which was induced by actin reorganization and three-dimensional (3D) cell-cell interactions among iHep cells. Similar to this situation, it is known that activation of Hippo signaling is important for hepatocytes to maintain their functionally differentiated state and liver homeostasis (Yimlamai et al., 2015; Yu et al., 2015). Through activation of the Hippo signaling pathway, liver-enriched transcription factors, especially Hnf1α, worked in iHep cell aggregates to induce the expression of transcriptional target genes related to functional properties of hepatocytes. Taken together, our findings may provide a new hepatic model using iHep cell aggregates that can be used as a tool to analyze the mechanisms of hepatocyte differentiation, investigate the pharmacological effects of drugs, and treat liver diseases by transplantation as an alternative to hepatocytes.

RESULTS

Cell Aggregation Culture Induces Growth Arrest and Functional Differentiation of iHep Cells
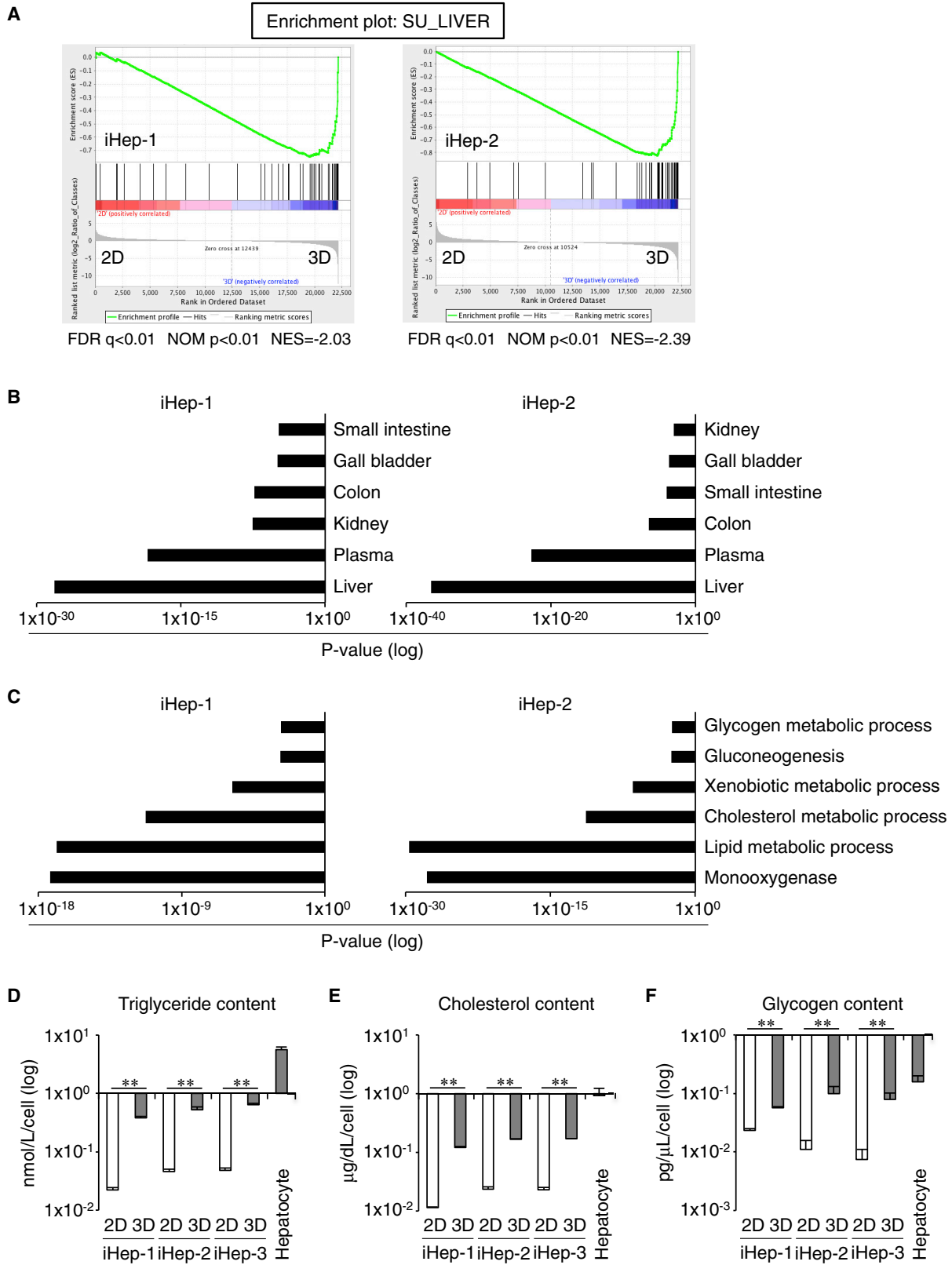
To examine whether iHep cells undergo hepatic maturation in cell-aggregation culture, we prepared iHep cells by inducing direct conversion of mouse dermal fibroblasts (MDFs) to iHep cells through overexpression of $Hnf4\alpha$ and $Foxa3$, as described previously (Figure S1A) (Miura and Suzuki, 2014; Sekiya and Suzuki, 2011). Immunofluorescence analyses revealed that iHep cells in monolayer cultures expressed the epithelial cell marker E-cadherin (E-cad) and the hepatocyte marker albumin (Alb) (Figure S1A). In addition, some iHep cells expressed the immature hepatic marker Afp (Figure S1A). Using these MDF-derived iHep cells, we conducted cell aggregation cultures of iHep cells and analyzed their characteristics in vitro. iHep cells were detached from type-I-collagen-coated culture dishes, dissociated into single cells, and inoculated into the wells of 6-well nonadherent cell culture plates containing 3,000 microholes in each well (Figure 1A). Under these culture conditions,

iHep cells formed uniform cell aggregates within 24 hr, and these aggregates were maintained in culture for more than 120 hr (Figure 1B). Similar to iHep cells in monolayer cultures, iHep cell aggregates expressed E-cad and Alb, while Afp expression was significantly decreased (Figures 1C and 1D). Western blot analyses revealed upregulation of cyclin-dependent kinase inhibitor p27 and downregulation of cyclin D1, D2, and D3 in iHep cell aggregates compared with the levels in iHep cell monolayer cultures (Figure 1D). Furthermore, phosphohistone H3 (pH3)-positive proliferating iHep cells were hardly detected in iHep cell aggregates (Figure S1B). Thus, cell-aggregate formation can rapidly cause iHep cells to lose their immature phenotype and undergo growth arrest.

Next, we examined whether cell-aggregation culture induces functional differentiation of iHep cells. The amounts of Alb and α-1-antitrypsin (Aat) or Afp, which were secreted from iHep cells into the culture medium, were significantly increased or decreased, respectively, in cell aggregation culture of iHep cells (Figure S1C). qPCR analyses also revealed that the expression levels of genes associated with hepatic functions, such as cytochrome P450 (Cyp) 1a2, 3a11, 3a13, Cyp7a1, and UDP-glucuronosyltransferase 1a1 (Ugt1a1), were significantly upregulated after formation of iHep cell aggregates (Figure 1E). Consistent with these results, the activities of Cyp1a2 and Cyp2c9 in iHep cell aggregates were markedly increased (Figure 1F). To induce efficient differentiation of iHep cells, each cell aggregate should be formed from 1,000–3,000 cells (Figures S1D–S1F). Moreover, the expression level of carbamoyl phosphate synthetase 1 (Cps1), encoding a rate-limiting enzyme of the urea cycle, was significantly increased in iHep cell aggregates (Figure 1E), and iHep cell aggregates produced a larger amount of urea from ammonia than iHep cell monolayer cultures (Figure 1G). In addition, carcinoembryonic antigen-related cell adhesion molecule 1 (Ceacam-1), whose expression marks bile canaliculi formation at the apical pole of hepatocytes in the liver, was expressed around the border of iHep cells composing cell aggregates (Figure S1G). Furthermore, 5- and 6-carboxy-2′,7′-dichlorofluorescein diacetate (carboxy-DCFDA) assays showed that the bile canaliculi-like structures appearing in iHep cell aggregates were functional (Figure S1H). These data demonstrate that iHep cells can acquire some properties of mature hepatocytes after cell-aggregate formation in our 3D culture conditions.

Figure 1. Growth Arrest and Hepatic Maturation of iHep Cells in Cell Aggregation Culture

(A) Schematic diagram of the experimental procedure. MDFs infected with retroviruses expressing $Hnf4\alpha$ and $Foxa3$ were directly converted into iHep cells. iHep cells were cultured under 3D culture conditions to induce cell-aggregate formation.

(B) Representative images of iHep cell aggregates 12, 24, 72, and 120 hr after initiation of 3D culture. The areas surrounded by the broken lines are enlarged in the middle panels. The right panels show representative images of H&E-stained iHep cell aggregates.

(C) Immunohistochemical staining of E-cad and co-immunofluorescence staining of E-cad with Alb or Afp were conducted on iHep cells 3 days after 3D culture initiation. DNA was stained with DAPI.

(D) Western blot analyses were conducted for 2D and 3D cultures of iHep cells. β-Actin was used for normalization. iHep cells were prepared from three independent experiments, designated iHep-1, iHep-2, and iHep-3.

(E) qPCR analyses were performed on total RNA from iHep cells in 2D cultures, iHep cells 5 days after 3D culture initiation, and hepatocytes freshly isolated from adult mouse livers. All data were normalized by the values for hepatocytes, and the fold differences are shown.

(F) Cyp1a2 and Cyp2c9 activities were measured in iHep cells in 2D cultures, iHep cells 5 days after 3D culture initiation, and hepatocytes cultured for 3 hr after isolation from adult mouse livers.

(G) The amounts of urea in culture media from iHep cells in 2D and 3D cultures and hepatocytes in 2D cultures were measured.

Scale bars represent 100 μm (B) and 40 μm (C). Data in (E)–(G) represent means ± SD (n = 3). *p < 0.05. **p < 0.01. See also Figure S1.

A Enrichment plot: SU_LIVER

iHep-1 — FDR q<0.01   NOM p<0.01   NES=-2.03

iHep-2 — FDR q<0.01   NOM p<0.01   NES=-2.39

B iHep-1 / iHep-2

C iHep-1 / iHep-2

D Triglyceride content

E Cholesterol content

F Glycogen content

(legend on next page)

Global Gene Expression Profiles and Functional Analyses Reveal Hepatic Maturation of iHep Cells in Cell Aggregation Culture

To further assess the hepatic maturation of iHep cells in cell aggregation culture, we investigated the global gene expression profiles in iHep cell aggregates and performed a gene set enrichment analysis (GSEA) using a set of genes specifically upregulated in human liver tissues. The data showed that the expression of human liver-specific genes was highly enriched in 3D cultures of iHep cell aggregates (Figure 2A). We extracted genes whose expression levels were more than twofold higher in iHep cell aggregates compared with those in iHep cell monolayer cultures and performed gene ontology (GO) enrichment analyses on these genes. The data revealed that the extracted genes were significantly enriched in genes expressed in the liver (Figure 2B). Moreover, these liver-enriched genes were related to hepatic functions associated with glucose metabolism, lipid metabolism, and drug metabolism (Figure 2C). We evaluated hepatic functions in iHep cell aggregates by measuring the contents of triglyceride, cholesterol, and glycogen and found that iHep cell aggregates became more functional than iHep cell monolayer cultures (Figures 2D–2F). Meanwhile, genes with more than twofold lower expression levels in iHep cell aggregates compared with those in iHep cell monolayer cultures were enriched in genes encoding cell-cycle-related proteins, suggesting the relevance of iHep cells in cell aggregation culture to growth arrest (Figure S2A).

Hepatic toxicities induced by high-dose administration of drugs are often recognized as one of the major problems occurring during treatment of diseases. We examined whether iHep cells exhibited drug-induced toxic sensitivities, similar to hepatocytes. Well-known drugs inducing hepatic toxicities, such as acetaminophen and amiodarone, were supplemented to iHep cell cultures. The data showed that iHep cell aggregates and primary hepatocytes exhibited similar sensitivities to drugs when compared with iHep cell monolayer cultures (Figure S2B). Collectively, these results indicate that cell aggregation culture can induce functional properties in iHep cells, which could enable the evaluation of hepatic functions using iHep cell aggregates *in vitro*.

Efficient Liver Tissue Reconstitution and Functional Hepatic Support by iHep Cell Aggregates Transplanted into the Livers of Fah^{−/−} Mice

The above data demonstrated that cell-aggregate formation by iHep cells can induce their functional differentiation in 3D cultures. Thus, we hypothesized that upon transplantation, iHep cell aggregates would function to reconstitute liver tissues more efficiently and rapidly than single iHep cells. To examine

this possibility, we directly transplanted iHep cell aggregates obtained from 3D cultures, single iHep cells dissociated from monolayer cultures, and hepatocytes freshly isolated from adult mouse livers into the median lobes of Fah^{−/−} mouse livers (Figure 3A). At 3 months after transplantation, iHep cell aggregates reconstituted liver tissues with higher and lower efficiency than single iHep cells and hepatocytes, respectively, by forming large colonies of Fah-positive donor-derived hepatocytes (Figures 3B and 3C). Interestingly, iHep cell aggregates engrafted in the liver reactivated their proliferative potential in response to regenerative signals in the Fah^{−/−} mouse liver, similar to transplanted hepatocytes (Figure 3D). Moreover, the iHep cell aggregate-derived hepatocytes formed bile canaliculi-like structures in the recipient mouse liver that were characterized by expression of Claudin-3, a member of the tight junction complex family, similar to hepatocytes in the wild-type mouse liver (Figure 3E). Thus, transplantation of iHep cell aggregates resulted in the engraftment and subsequent proliferation of donor-derived cells with the normal morphology of hepatocytes.

To evaluate the functional efficiency of transplanted iHep cell aggregates, we compared the survival rates of recipient mice after transplantation of MDFs, single iHep cells, iHep cell aggregates, and hepatocytes into the median lobes of Fah^{−/−} mouse livers (Figure 3F). Survival curves revealed a significant increase in the lifespan of the recipient mice transplanted with iHep cell aggregates, while hepatocyte transplantation resulted in the most efficient recovery of mice (Figure 3G). Collectively, iHep cell aggregates allowed efficient liver tissue reconstitution and provided functional hepatic support after transplantation into the injured mouse liver.

Hippo Signaling Is Activated in iHep Cells during Formation of Cell Aggregates

Although cell aggregation culture induced growth arrest and hepatic maturation of iHep cells, the mechanisms responsible for these phenomena have remained unknown. To identify the signaling molecules involved in this process, we performed a GSEA using a set of genes related to oncogenic signatures, because the growth potential of iHep cells was strikingly different between monolayer culture and cell aggregation culture. Among the sets of genes showing differential expression between the two distinct culture conditions of iHep cells, we focused on a gene set associated with Yes-associated protein (Yap), a central effector molecule of the Hippo signaling pathway (Figure 4A). In general, it is known that activated Hippo signaling results in phosphorylation of Yap and that phosphorylated Yap (pYap) is localized in the cytoplasm, where it undergoes proteasomal degradation (Yimlamai et al., 2015; Yu et al., 2015). When Hippo

---

Figure 2. Global Gene Expression Profiles and Functional Properties of iHep Cell Aggregates

(A) A GSEA of microarray data for iHep cells in 2D and 3D cultures was performed using a set of genes specifically upregulated in human liver tissues (gene set name: SU_LIVER).

(B and C) GO enrichment analyses were performed for genes whose expression levels were more than twofold higher in iHep cell aggregates than in iHep cell monolayer cultures (B). The liver-enriched genes shown in (B) were related to hepatic functions associated with glucose metabolism, lipid metabolism, and drug metabolism (C).

(D–F) Amounts of triglyceride (D), cholesterol (E), and glycogen (F) in 2D and 3D cultures of iHep cells and hepatocytes freshly isolated from adult mouse livers were measured. Data represent means ± SD (n = 3). **p < 0.01.
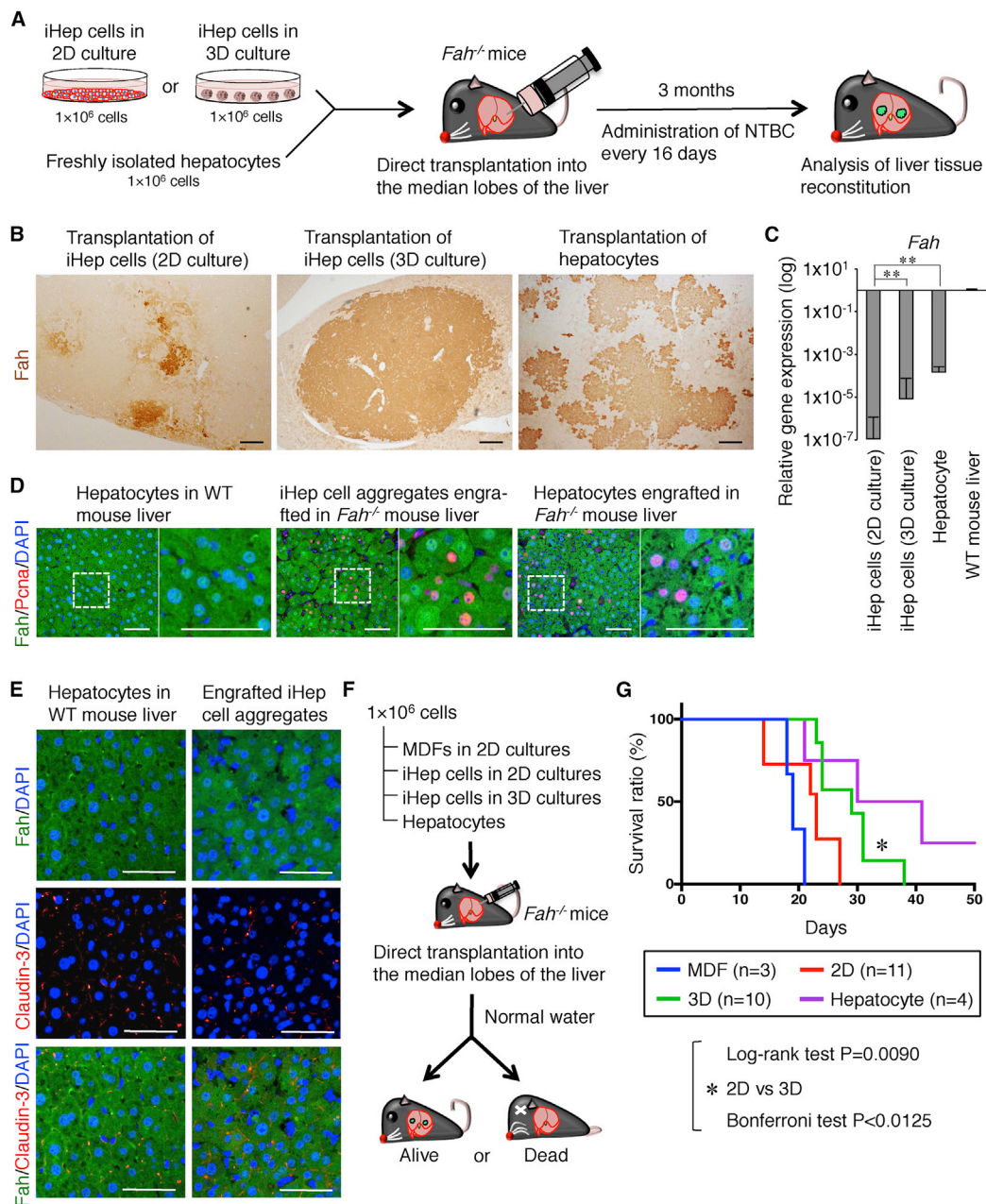
See also Figure S2.

Figure 3. iHep Cell Aggregates Efficiently Reconstitute Liver Tissues and Support Hepatic Function after Transplantation

(A) Schematic diagram of the experimental procedure. At 3 months after transplantation, the median lobes of $Fah^{-/-}$ mouse livers were analyzed.

(B) Immunohistochemical staining of Fah was conducted on the livers of $Fah^{-/-}$ mice 3 months after transplantation of hepatocytes or iHep cells obtained from 2D and 3D cultures.

(C) qPCR analyses of Fah were carried out on total RNA from the livers of wild-type (WT) mice and $Fah^{-/-}$ mice transplanted with hepatocytes or iHep cells obtained from 2D and 3D cultures. All data were normalized by the values for WT mouse livers, and the fold differences are shown. Data represent means ± SD (n = 3). **p < 0.01.

(D) Co-immunofluorescence staining of Fah with proliferating cell nuclear antigen (Pcna) was conducted for the livers of WT mice and $Fah^{-/-}$ mice transplanted with iHep cell aggregates or hepatocytes. The areas surrounded by the broken lines are enlarged in the right panels.

(E) Co-immunofluorescence staining of Fah with Claudin-3 was conducted for the livers of WT mice and $Fah^{-/-}$ mice transplanted with iHep cell aggregates.

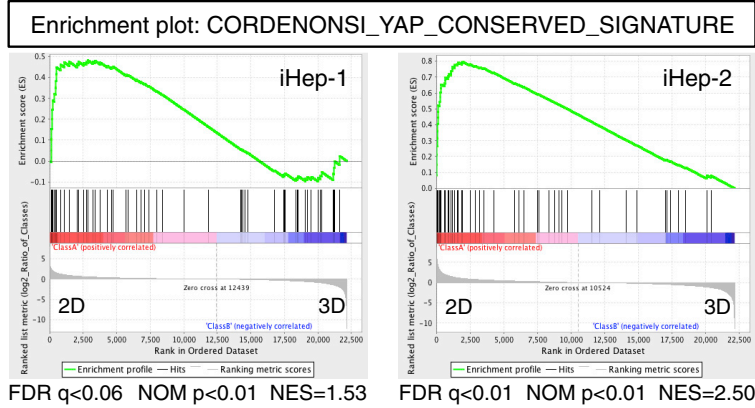(F) Schematic diagram of the experimental procedure.

(G) Kaplan-Meier survival curves of $Fah^{-/-}$ mice after transplantation of MDFs (n = 3), iHep cells obtained from 2D (n = 11) and 3D (n = 10) cultures, and hepatocytes (n = 4). Statistical analyses using the Bonferroni method revealed a significant difference between the curves for iHep cells obtained from 2D and 3D cultures.

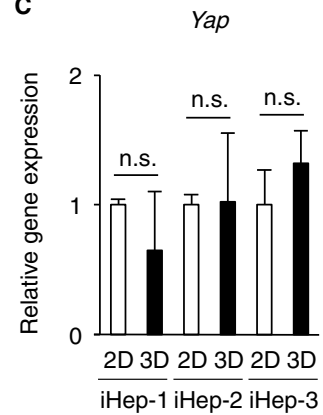DNA was stained with DAPI (D and E). Scale bars represent 200 μm (B) and 50 μm (D and E).

A

iHep-1

C6 oncogenic signatures

iHep-2

NAME	NES	NOM p-val	FDR q-val
RPS14_DN.V1_DN	1.6785823	0	0.026681723
CSR_LATE_UP.V1_UP	1.5957901	0	0.037009653
CORDENONSI_YAP_CONSERVED_SIGNATURE	1.5328431	0.002994012	0.052036975
GCNP_SHH_UP_LATE.V1_UP	1.4995422	0	0.05432136
E2F1_UP.V1_UP	1.4524211	0.004854369	0.071293056
PRC2_EZH2_UP.V1_UP	1.4235982	0.004651163	0.07932487
VEGF_A_UP.V1_DN	1.3999774	0.017699115	0.083526224
GCNP_SHH_UP_EARLY.V1_UP	1.3406878	0.025125628	0.13042332
RB_DN.V1_DN	1.2958113	0.02734375	0.17648962
BMI1_DN_MEL18_DN.V1_UP	1.2628524	0.031111112	0.21386445

NAME	NES	NOM p-val	FDR q-val
CORDENONSI_YAP_CONSERVED_SIGNATURE	2.5006506	0	0
RPS14_DN.V1_DN	2.4557369	0	0
RB_P107_DN.V1_UP	2.2790353	0	0
GCNP_SHH_UP_LATE.V1_UP	2.2338562	0	0
CSR_LATE_UP.V1_UP	2.228808	0	0
E2F1_UP.V1_UP	2.146438	0	0
ERB2_UP.V1_DN	2.1254385	0	0
VEGF_A_UP.V1_DN	2.0587547	0	0
PRC2_EZH2_UP.V1_UP	1.9086616	0	1.40E−04
RB_DN.V1_UP	1.8503664	0	6.63E−04

B

Enrichment plot: CORDENONSI_YAP_CONSERVED_SIGNATURE

FDR q<0.06   NOM p<0.01   NES=1.53

FDR q<0.01   NOM p<0.01   NES=2.50

C

Yap

D

Yap/DAPI

E

pYap/Yap ratio

F

Ctgf

Cyr61
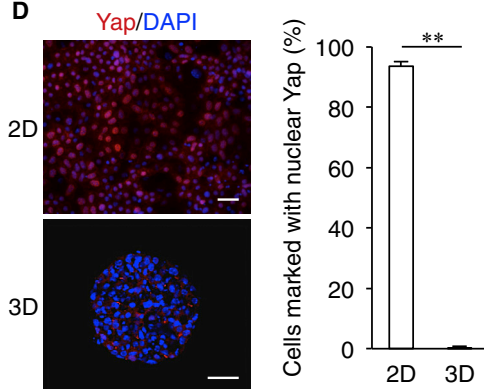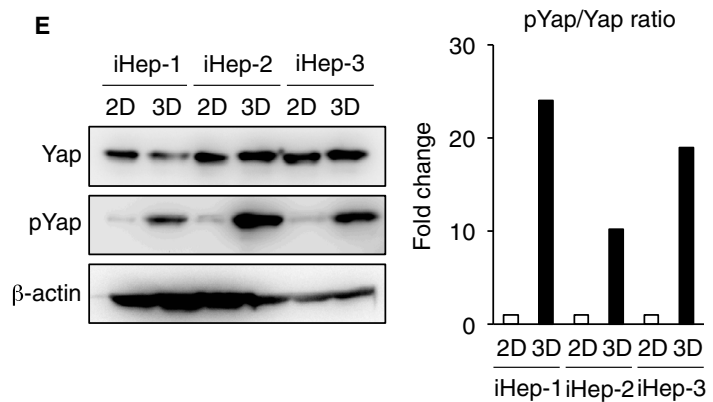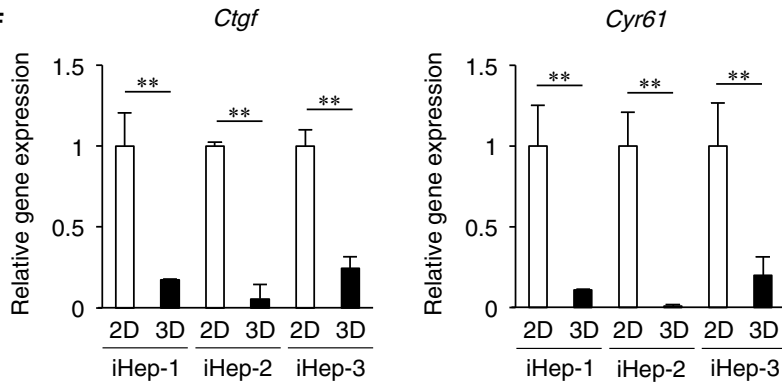
signaling is inactivated, Yap acts as a transcription coactivator and exerts its transcriptional activity by interacting with the TEA domain (Tead) family of transcriptional factors, often leading to cell-cycle progression of cells (Yimlamai et al., 2015; Yu et al., 2015). In liver development and homeostasis, suitable activation and inactivation of Hippo signaling are essential for the regulation of proliferation and differentiation of hepatic lineage cells (Lee et al., 2016; Yimlamai et al., 2014). In particular, inactivation of Hippo signaling allows transcriptional activation of Yap target genes in hepatocytes and induces their dedifferentiation and proliferation (Lee et al., 2016; Yimlamai et al., 2014). Consistently, the present data demonstrated that the expression levels of Yap-associated genes were upregulated in proliferating iHep cells in monolayer cultures compared with the growth-arrested iHep cells in cell aggregation cultures (Figure 4B). Although the expression levels of the Yap gene did not differ significantly between monolayer culture and cell aggregation culture of iHep cells, Yap protein was specifically accumulated in the nucleus of iHep cells proliferating in monolayer cultures (Figures 4C and 4D). Moreover, in iHep cell aggregates, the amounts of pYap were relatively increased, and the expression levels of Yap target genes connective tissue growth factor (*Ctgf*) and cysteine rich-61 (*Cyr61*) were significantly downregulated (Figures 4E and 4F). These data demonstrated that Hippo signaling inactivated in monolayer cultures of iHep cells can be activated in iHep cell aggregates under 3D culture conditions, suggesting that cytoplasmic localization and subsequent degradation of pYap in iHep cell aggregates led to growth arrest and hepatic maturation of iHep cells.

Constitutive Yap Activation Blocks Growth Arrest and Hepatic Maturation of iHep Cells in Cell Aggregation Culture

To examine whether Yap inactivation is critical for growth arrest and functional differentiation of iHep cells in cell aggregation culture, we overexpressed two types of constitutively active forms of Yap, 5SA and 5SA/S94A, in iHep cell aggregates (Figure 5A). In the 5SA mutant of Yap, five serine residues that act as phosphorylation target sites for large tumor suppressor kinases (Lats) were replaced with alanine, leading to constitutive activation of Yap in the cell nucleus (Zhao et al., 2007). The other mutant form of Yap, 5SA/S94A, has an additional mutation to the 5SA mutant that inhibits interactions with Tead transcriptional factors (Zhao et al., 2008). iHep cells overexpressing 5SA and 5SA/S94A, designated iHep-5SA and iHep-5SA/S94A cells, respec-

tively, formed larger and flatter cell aggregates compared with those formed by mock-infected iHep cells (Figure 5B). However, the cell aggregates formed by iHep-5SA and iHep-5SA/S94A cells were easily dissociated by simple pipetting, indicating that intercellular adhesion among these iHep cells was much weaker than that among mock-infected iHep cells (Figure 5B). Although the morphologies in the cell aggregates formed by iHep-5SA and iHep-5SA/S94A cells were similar, the growth ability was only activated in iHep-5SA cells, suggesting that the interaction between Yap and Teads was required for the proliferation of iHep cells (Figure 5C). Moreover, the expression levels of *Cyp1a2*, *Cyp7a1*, and *Ugt1a1* and the activities of Cyp1a2 and Cyp2c9 in iHep-5SA cell aggregates were much lower than those in mock-infected iHep cell aggregates, while these inhibitory effects for hepatic maturation in iHep-5SA cell aggregates were partially recovered in iHep-5SA/S94A cell aggregates (Figures 5D and 5E). Thus, these results suggested that Yap-mediated inhibition of iHep cell maturation was regulated, at least in part, by a Tead-dependent regulatory mechanism. Taken together, our data demonstrate that Yap inactivation in iHep cells was required for the typical cell-aggregate formation and subsequent induction of growth arrest and hepatic maturation of iHep cells in cell-aggregation culture.

To further test the importance of Yap inactivation in functional differentiation of iHep cells, we conducted qPCR analyses of iHep cells expressing a short hairpin RNA (shRNA) against Yap and compared the results with those in iHep cells transduced with a lentiviral vector containing a control shRNA under two-dimensional (2D) culture conditions. The data showed that suppression of Yap expression in iHep cells significantly decreased and increased the expression level of *Afp* and those of *Alb*, *G6P*, *Cyp1a2*, and *Cyp7a1*, respectively, compared with iHep cells expressing a control shRNA, while the efficacy of Yap inhibition in iHep cell monolayer cultures was lower than that of cell-aggregate formation of iHep cells (Figure S3). These data suggest that although Yap inactivation is essential for functional differentiation of iHep cells, hepatic tissue-like structures formed by aggregation of iHep cells is also required for more efficient differentiation of iHep cells.

Yap Inactivation in iHep Cell Aggregates Is Regulated by Intracellular Actin Reorganization, Intercellular Adhesion, and Humoral Factors in the Culture Medium

In the following experiments, we attempted to identify the upstream signals of Yap inactivation in iHep cell aggregates.

Figure 4. Hippo Signaling Is Activated in iHep Cell Aggregates

(A and B) A GSEA of microarray data for iHep cells in 2D and 3D cultures was performed using a set of genes related to oncogenic signatures. Gene sets associated with Yap are highlighted by the red squares (A). Yap-associated genes were upregulated in 2D cultures of iHep cells compared with 3D cultures of iHep cells (B).

(C) qPCR analyses were performed on total RNA from iHep cells in 2D cultures and iHep cells 5 days after 3D culture initiation.

(D) Immunofluorescence staining of Yap was conducted for iHep cells in 2D cultures and iHep cells 5 days after 3D culture initiation. The right graph shows the percentages of cells marked with nuclear Yap in 2D and 3D cultures of iHep cells (500–1,000 cells were counted in 2D and 3D cultures of iHep cells). DNA was stained with DAPI. Scale bars, 40 μm.

(E) Western blot analyses were conducted for iHep cells in 2D cultures and iHep cells 5 days after 3D culture initiation. β-Actin was used for normalization. The right graph shows quantification of western blotting data for pYap/YAP ratios in 2D and 3D cultures of iHep cells.

(F) qPCR analyses were performed on total RNA from iHep cells in 2D cultures and iHep cells 5 days after 3D culture initiation.

All data were normalized by the values for iHep cells in 2D cultures, and the fold differences are shown (C, E, and F). Data in (C), (D), and (F) represent means ± SD (n = 3). **p < 0.01; n.s., not significant.
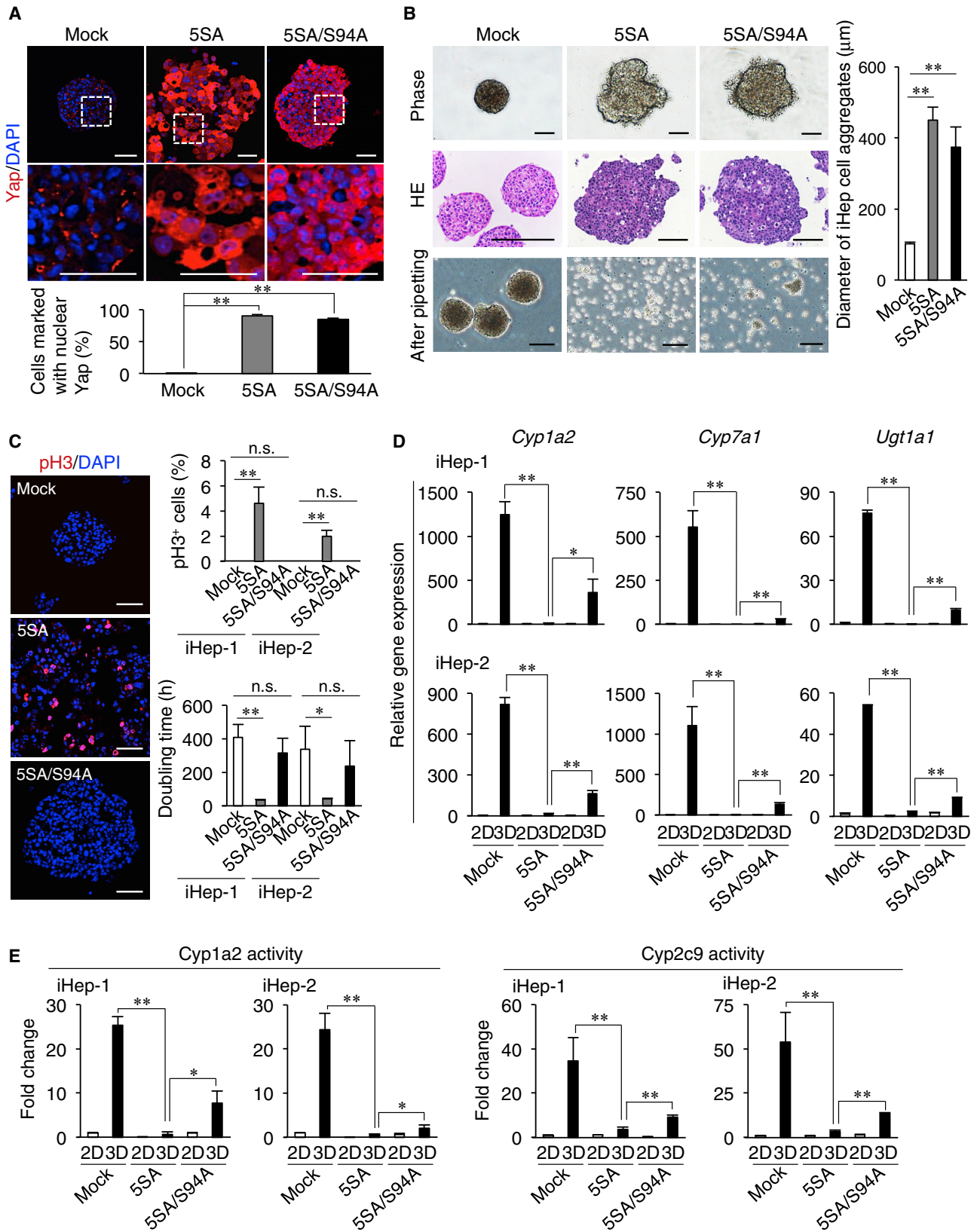
(legend on next page)

Previous studies have demonstrated that actin reorganization affects pYap degradation and is necessary for cell-aggregate formation by rat hepatocytes (Aragona et al., 2013; Tzanakakis et al., 2001). These observations suggested that intracellular actin reorganization may also be effective for Yap inactivation in iHep cell aggregates. To examine this possibility, we treated iHep cells with the actin polymerization inhibitor cytochalasin D (Cyto D) and the actin depolymerization inhibitor jasplakinolide (Jas) during cell-aggregate formation. Yap was normally inactivated in iHep cells at 1 day after initiation of cell aggregation culture (Figure 6A). Cyto D treatment inhibited both Yap inactivation and cell-aggregate formation of iHep cells, while iHep cells treated with Jas formed cell aggregates but did not inactivate Yap (Figure 6A). Cyto D and Jas-treated iHep cells, the expression levels of *Cyp1a2* and *Cyp7a1* were much lower than those in control iHep cells (Figure 6B). Thus, actin polymerization in iHep cells is initially required for cell-aggregate formation, while subsequent actin depolymerization in iHep cells is required to inactivate Yap and induce hepatic maturation of iHep cells. In addition to intracellular actin reorganization, we investigated the role of intercellular adhesion in Yap inactivation during cell-aggregate formation by iHep cells. As E-cad was ubiquitously expressed in the intercellular regions of iHep cell aggregates, we treated iHep cells with EDTA, which chelated calcium and thereby inhibited E-cad-mediated intercellular adhesion during cell-aggregate formation. The data showed that EDTA-treated iHep cells were unable to either form cell aggregates or inactivate Yap (Figure 6C). Moreover, the expression levels of *Cyp1a2* and *Cyp7a1* in EDTA-treated iHep cells were much lower than those in control iHep cells (Figure 6D). Thus, E-cad-mediated intercellular adhesion of iHep cells is required for inhibition of Yap and induction of hepatic maturation of iHep cells in cell aggregation culture. In addition, because growth factors (GFs) and fetal bovine serum (FBS) are known to activate Yap (Fan et al., 2013; Yu et al., 2012), we examined whether GFs and FBS can inhibit Yap inactivation in iHep cell aggregates. iHep cells treated with hepatocyte growth factor (HGF) and epidermal growth factor (EGF) and/or a high dose of FBS (10%) in the medium formed cell aggregates that were morphologically similar to those formed from iHep cells cultured in the standard 3D culture medium containing only a low dose of FBS (0.5%) in the medium (Figure 6E). We found that Yap inhibition in iHep cell aggregates was strongly inhibited in culture with GFs and/or a high dose of

FBS (Figure 6E). In the presence of GFs and/or a high dose of FBS, the expression levels of *Cyp1a2* and *Cyp7a1* were significantly suppressed in iHep cell aggregates (Figure 6F). Collectively, intracellular actin reorganization, intercellular adhesion, and depletion of GFs and FBS from the culture medium were indispensable for inactivating Yap and inducing functional differentiation of iHep cells in cell aggregation culture.

Hnf1α Expression Upregulated by Yap Inactivation in iHep Cell Aggregates Is Required for Hepatic Maturation of iHep Cells

Finally, we sought to clarify the mechanism underlying iHep cell maturation induced by Yap inactivation in iHep cell aggregates. As transcription factors generally play fundamental roles in the regulation of cell differentiation, we performed a GSEA using a set of genes whose expression was regulated by specific transcription factors. The data showed that the genes exhibiting differential expression between monolayer culture and cell aggregation culture of iHep cells were enriched in many sets of genes regulated by transcription factors responsible for hepatocyte differentiation (Figure 7A). Among them, a set of genes transcriptionally regulated by Hnf1 exhibited the largest change between the two culture conditions of iHep cells. The expression of Hnf1 target genes was significantly upregulated in iHep cells forming cell aggregates compared with iHep cells in monolayer cultures (Figure 7B). The Hnf1 family of transcription factors contains two major isoforms, Hnf1α and Hnf1β. Although both Hnf1 isoforms are expressed in the liver, Hnf1α is mainly expressed in hepatocytes and has critical roles in the differentiation and function of these cells (Lee et al., 1998; Shih et al., 2001). Thus, it is suggested that an increase in transcriptional regulation by Hnf1α is important for hepatic maturation of iHep cells in cell aggregation culture.

The data obtained from qPCR and chromatin immunoprecipitation followed by qPCR (ChIP-qPCR) showed that the expression levels of pyruvate kinase (*Pklr*), plasminogen (*Plg*), and glucose-6-phosphatase (*G6P*), Hnf1α target genes expressed in mature hepatocytes, were significantly upregulated in iHep cell aggregates through increased recruitment of Hnf1α to the promoter regions of these genes (Figures S4A and S4B). The enhanced transcriptional activity of Hnf1α in iHep cell aggregates suggested upregulation of *Hnf1α* expression in iHep cells. Indeed, qPCR analyses revealed that the expression levels of

Figure 5. Inhibition of Growth Arrest and Hepatic Maturation of iHep Cell Aggregates by Constitutive Activation of Yap
(A) Immunofluorescence staining of Yap was conducted on mock-infected iHep, iHep-5SA, and iHep-5SA/S94A cells 5 days after 3D culture initiation. The areas surrounded by the broken lines are enlarged in the lower panels. The bottom graph shows the percentages of cells marked with nuclear Yap in 3D cultures of the indicated cell types (400–800 cells were counted for each cell type).
(B) Representative morphologies and H&E staining images of the indicated cell types 5 days after 3D culture initiation. The bottom panels show the 3D cultures of three cell types just after pipetting. The right graph shows the diameters of cell aggregates formed by the indicated cell types (24 cell aggregates were analyzed for each cell type, and means ± SD are shown).
(C) Immunofluorescence staining of pH3 was conducted on the indicated cell types 5 days after 3D culture initiation. The upper right graph shows the percentages of pH3-positive cells in the indicated cell types at 5 days after 3D culture initiation (600–1,200 cells were counted for each cell type of iHep-1 and iHep-2). The lower right graph shows the doubling times of the indicated cell types from days 1–3 of 3D culture.
(D) qPCR analyses were performed on total RNA from the indicated cell types in 2D cultures and the same cell types at 5 days after 3D culture initiation.
(E) Cyp1a2 and Cyp2c9 activities were measured in the indicated cell types in 2D cultures and the same cell types at 5 days after 3D culture initiation.
DNA was stained with DAPI (A and C). Scale bars represent 100 μm (B) and 40 μm (A and C). All data were normalized by the values for mock-infected iHep cells in 2D cultures, and the fold differences are shown (D and E). Data in (A) and (C)–(E) represent means ± SD (n = 3). *p < 0.05; **p < 0.01; n.s., not significant. See also Figure S3.
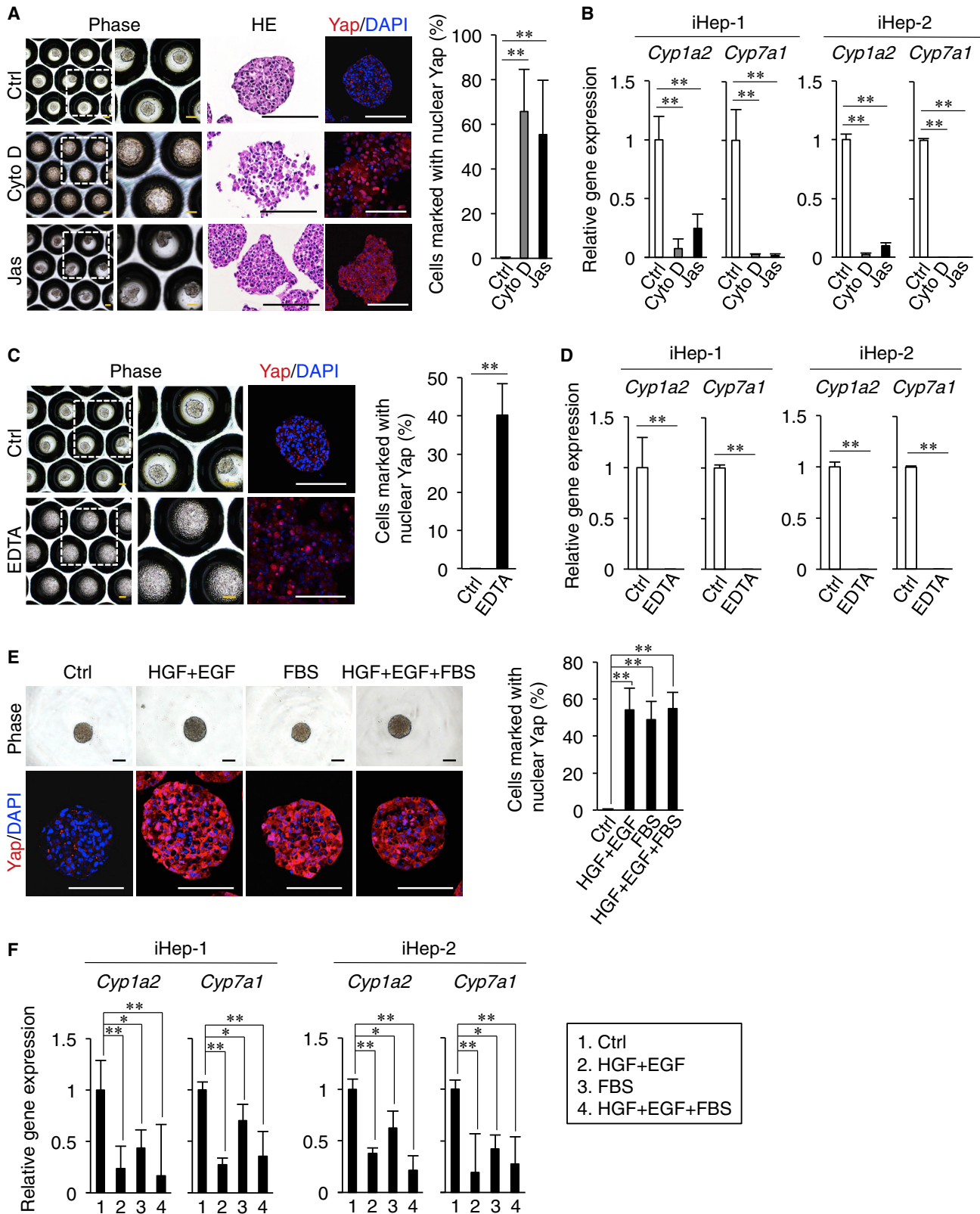
(legend on next page)

Hnf1α in iHep cell aggregates were significantly increased compared with those in iHep cell monolayer cultures (Figure 7C). To examine whether the increase in *Hnf1α* expression in iHep cell aggregates is required for hepatic maturation of iHep cells, we conducted qPCR analyses of iHep cells expressing an shRNA against Hnf1α and compared the results with those in iHep cells expressing a control shRNA. The data showed that suppression of Hnf1α expression in iHep cell aggregates reduced the expression levels of *Cyp7a1* and *Ugt1a1*, as well as those of *Pklr*, *Plg*, and *G6P*, in iHep cells (Figure 7D). In contrast, overexpression of *Hnf1α* in iHep cells increased the expression levels of not only *Plg* and *G6P* but also *Cyp1a2*, *Cyp7a1*, and *Ugt1a1*, even under 2D culture conditions (Figures S5A and S5B). However, cell aggregation culture allowed more efficient differentiation of iHep cells (Figure S5B), suggesting that other mechanisms were involved in iHep cell maturation during cell-aggregate formation. Indeed, the expression levels of *Ahr* and *Car*, both of which play an important role during hepatic differentiation from ESCs (Takayama et al., 2013), were significantly upregulated in iHep cell aggregates (Figure S5C). It is known that these nuclear receptors regulate the expression of *Cyp* genes (Honkakoski and Negishi, 2000), and it has been suggested that Hnf1α is associated with Ahr activation (Oshida et al., 2015). These data demonstrate that upregulation of *Hnf1α* expression as well as Hnf1α target gene expression in iHep cell aggregates led to functional differentiation of iHep cells in cooperation with other factors responsible for hepatocyte maturation.

We investigated the relationship between inactivation of Yap and upregulation of *Hnf1α* expression in iHep cell aggregates. qPCR analyses revealed that upregulation of *Hnf1α* expression and Hnf1α target gene *Pklr*, *Plg*, and *G6P* expression was significantly suppressed in iHep-5SA cell aggregates, while the suppression was partially rescued in iHep-5SA/S94A cell aggregates (Figure 7E). Simultaneously, recruitment of Hnf1α to the promoter regions of the Pklr, Plg, and G6P genes was significantly decreased in iHep-5SA cell aggregates and partially recovered in iHep-5SA/S94A cell aggregates (Figure S4C). Moreover, shRNA-mediated Yap inhibition in iHep cell monolayer cultures induced upregulation of *Hnf1α* expression (Figure S3B). Thus, Yap inactivation in iHep cell aggregates was essential for upregulation of *Hnf1α* expression, and Yap-mediated inhibition of *Hnf1α* expression was controlled, at least in

part, in a Tead-dependent manner. To clarify the mechanism underlying the upregulation of *Hnf1α* expression in iHep cell aggregates, we investigated the transcriptional regulation of *Hnf1α* expression by the Yap-Tead complex. We searched for a Tead-binding motif (CATTCCT) in the Hnf1α promoter region within ±2 kb from the transcription starting site (TSS) using the JASPAR database and found two specific regions with predicted Tead-binding motifs, designated R2 and R3 (Figure 7F). ChIP-qPCR analyses revealed that Yap was recruited to R2, but not R3, indicating that the Yap-Tead complex could bind to R2 in the Hnf1α promoter region (Figure 7G). When the Yap-Tead complex acts as a transcriptional repressor for its target genes, chromodomain helicase DNA-binding protein 4 (Chd4), a subunit of the nucleosome remodeling and deacetylase transcriptional repressor complex, is often recruited cooperatively (Kim et al., 2015; Lee et al., 2016). Thus, we examined whether Chd4 was recruited to the regions bound by the Yap/Tead complex to suppress the expression of *Hnf1α*. ChIP-qPCR analyses showed that Chd4 bound to R2, but not R3, in the Hnf1α promoter region (Figure 7G). Thus, the transcriptional repressor unit composed the Yap/Tead complex and Chd4 suppressed *Hnf1α* expression in iHep cells, and Yap inactivation in iHep cell aggregates led to upregulation of *Hnf1α* expression and subsequent hepatic maturation of iHep cells (Figure 7H). To confirm these findings, we introduced the 5SA mutant of Yap into mouse hepatocytes *in vivo*. Hepatocytes overexpressing 5SA, designated Hep-5SA, had an abnormal morphology and were surrounded by inflammatory cells in the liver (Figures S6A and S6B). In Hep-5SA cells, the expression levels of Yap target genes *Ctgf* and *Cyr61* were increased, while those of *Hnf1α* and Hnf1α target genes *Pklr*, *Plg*, and *G6P* were decreased (Figures S6C and S6D), indicating that Yap activation can inhibit *Hnf1α* expression in hepatocytes and iHep cells.

DISCUSSION

In this study, we found that cell aggregation culture of iHep cells can facilitate their differentiation into functional hepatocytes through activation of the Hippo signaling pathway. Under 3D culture conditions, iHep cells obtained from monolayer cultures initially polymerize and subsequently depolymerize intracellular actin filaments and simultaneously form cell aggregates through

Figure 6. Regulatory Mechanisms for Yap Inactivation in iHep Cell Aggregates

(A) Representative morphologies, H&E staining images, and Yap immunostaining images of iHep cells 1 day after 3D culture initiation with or without Cyto D or Jas. The areas surrounded by the broken lines are enlarged in the second left panels. The right graph shows the percentages of cells marked with nuclear Yap in 3D cultures of iHep cells with or without Cyto D or Jas (400–500 cells were counted for control, Cyto-D-treated, and Jas-treated iHep cells).

(B) qPCR analyses were performed on total RNA from control, Cyto-D-treated, and Jas-treated iHep cells 1 day after 3D culture initiation.

(C) Representative morphologies and Yap immunostaining images of iHep cells 1 day after 3D culture initiation with or without EDTA. The areas surrounded by the broken lines are enlarged in the middle panels. The right graph shows the percentages of cells marked with nuclear Yap in 3D cultures of iHep cells with or without EDTA (400–500 cells were counted for control and EDTA-treated iHep cells).

(D) qPCR analyses were performed on total RNA from control and EDTA-treated iHep cells 1 day after 3D culture initiation.

(E) Representative morphologies and Yap immunostaining images of iHep cells 5 days after 3D culture initiation with or without HGF and EGF and/or a high dose of FBS. The right graph shows the percentages of cells marked with nuclear Yap in 3D cultures of iHep cells with or without HGF and EGF and/or a high dose of FBS (400–700 cells were counted for control, HGF/EGF-treated, FBS-treated, and HGF/EGF/FBS-treated iHep cells).

(F) qPCR analyses were performed on total RNA from control, HGF/EGF-treated, FBS-treated, and HGF/EGF/FBS-treated iHep cells 5 days after 3D culture initiation.

DNA was stained with DAPI (A, C, and E). Scale bars, 100 μm (A, C, and E). All data were normalized by the values for control iHep cells, and the fold differences are shown (B, D, and F). Data represent means ± SD (n = 3). *p < 0.05; **p < 0.01.
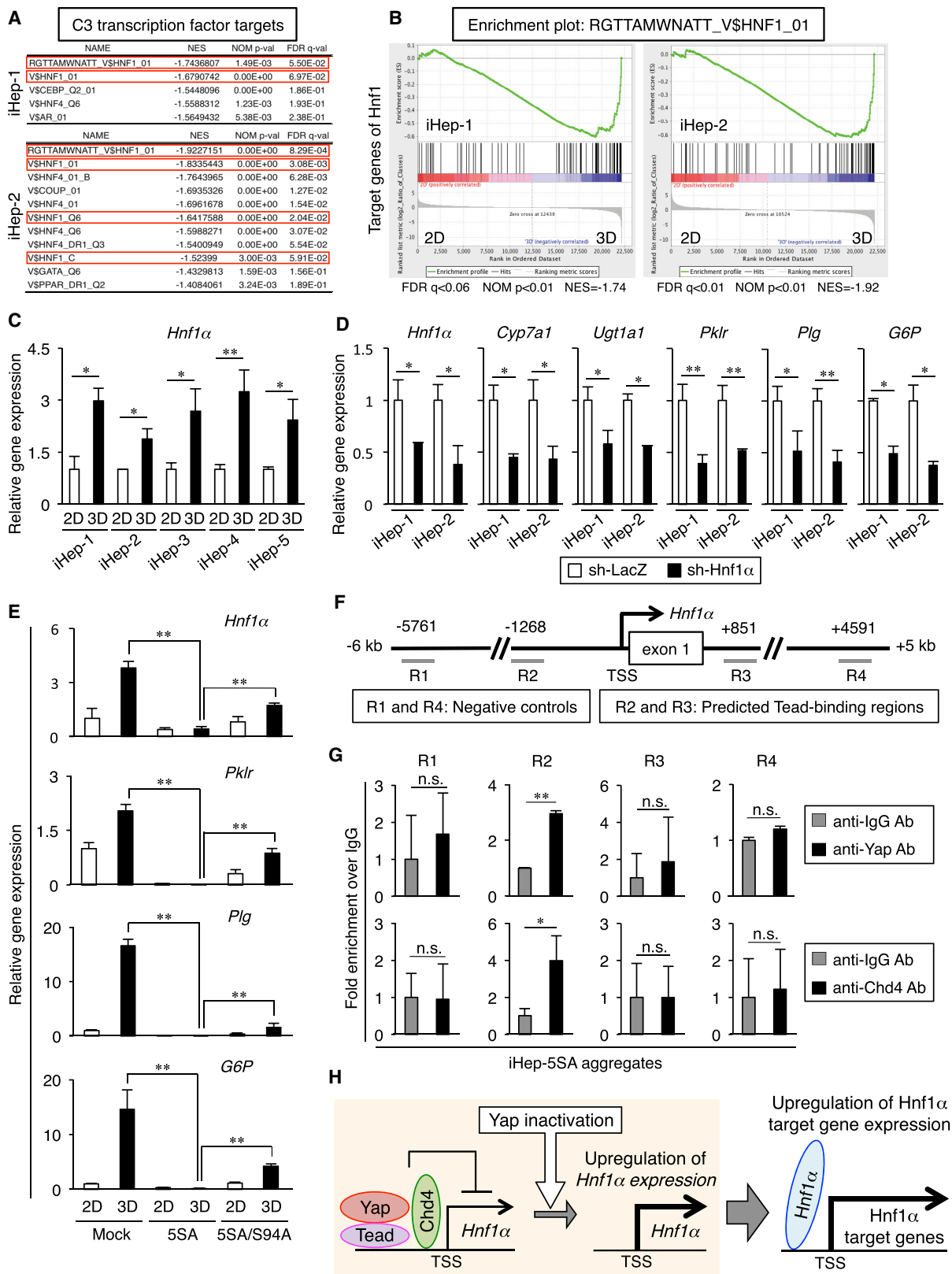
E-cad-mediated intercellular adhesion. These serial steps in the formation of iHep cell aggregates are critical for induction of Yap inactivation in iHep cells. Meanwhile, although GFs and FBS allow cell-aggregate formation of iHep cells, Yap inactivation in iHep cell aggregates is inhibited in the presence of GFs and FBS. After inactivation of Yap, iHep cells undergo growth arrest and functional differentiation through downregulation of cell-cycle-related gene expression and upregulation of liver-enriched gene expression in cell aggregation culture. Mainly, Hnf1α, whose mRNA expression is increased in iHep cell aggregates in the absence of direct inhibition by the Yap/Tead/Chd4 transcriptional repressor unit, acts as a central transcription factor that regulates the expression of liver-enriched genes in iHep cell aggregates.

Cell aggregation culture is a well-established culture system that promotes hepatic maturation of primary hepatocytes and hepatocyte-like cells derived from ESCs and iPSCs, as well as iHep cells. However, it has not been shown that cell-aggregate transplantation can be available for functional reconstitution of injured liver tissues. The present data demonstrate that growth-arrested iHep cells in cell aggregation culture reactivate their proliferative potential and efficiently reconstitute liver tissues in $Fah^{-/-}$ mice after transplantation. Moreover, $Fah^{-/-}$ mice transplanted with iHep cell aggregates live longer than those transplanted with iHep cells from monolayer cultures. Thus, cell-aggregate transplantation will be a more suitable clinical strategy for reconstitution of injured liver tissues than transplantation of dissociated cells.

Hepatic maturation of iHep cells in cell aggregation cultures requires upregulation of $Hnf1α$ expression as a result of Yap inactivation in iHep cells. A previous study showed that Yap activation induced by loss of $Lats1/2$ in mouse hepatocytes led to downregulation of $Hnf4α$ expression and transdifferentiation into biliary lineage cells (Lee et al., 2016). Similar to the mechanism for suppression of $Hnf1α$ expression in iHep cells, Yap-mediated downregulation of $Hnf4α$ expression in hepatocytes is regulated by the Yap/Tead/Chd4 transcriptional repressor unit (Lee et al., 2016). Thus, it is suggested that the transcriptional activity of Hnf4α in iHep cell aggregates is increased compared with that in iHep cell monolayer cultures. Indeed, the expression levels of liver-enriched genes regulated by transcription factors responsible for hepatocyte differentiation, including Hnf1, Hnf4, CCAAT/enhancer-binding protein, and Gata, are increased in iHep cell aggregates. These results suggest that in addition to Hnf1α, Yap can widely inhibit the expression of transcription factors that regulate hepatocyte differentiation in iHep cells and allow their proliferation. Although inactivation of Yap and upregulation of $Hnf1α$ expression are essential for hepatic maturation of iHep cells in cell aggregation cultures, shRNA-mediated Yap inhibition and overexpression of $Hnf1α$ in iHep cell monolayer cultures can only induce partial differentiation of iHep cells compared with the formation of iHep cell aggregates. Thus, inactivation of Yap and upregulation of $Hnf1α$ expression may be required, but not sufficient, to induce functional differentiation of iHep cells, and other stimuli caused by the formation of cell aggregates may also be required for more efficient differentiation of iHep cells. Moreover, the present data demonstrate that Yap-mediated inhibition of iHep cell maturation is mainly, but not completely, regulated in a Tead-dependent manner. Thus, a Tead-independent regulatory mechanism may also contribute to inhibition of the hepatic maturation of iHep cells. As Yap can bind to transcription factors other than Teads (Hansen et al., 2015; Mauviel et al., 2012), Yap may also bind to other transcription factors to inhibit the hepatic maturation of iHep cells.

iHep cells are potentially useful for basic studies and medical applications, including pathological analyses of liver diseases, cell-based transplantation therapies, development of bio-artificial liver support devices, and screening of pharmacological effects of drugs. However, the immature phenotype of iHep cells has made it difficult to consider their applications. As shown in the present study, cell-aggregate formation enables rapid induction of functional differentiation of iHep cells, suggesting that iHep cell aggregates can be used in medical applications as an alternative to hepatocytes. Thus, our findings may provide insights into basic research and potential therapies for liver diseases.

Figure 7. Yap Inactivation in iHep Cell Aggregates Upregulates *Hnf1α* Expression to Induce Hepatic Maturation of iHep Cells

(A and B) GSEA of microarray data for iHep cells in 2D and 3D cultures was performed using a set of genes whose expression was regulated by specific transcription factors. Gene sets associated with Hnf1 are highlighted by the red squares (A). Hnf1-associated genes were upregulated in 3D cultures of iHep cells compared with 2D cultures of iHep cells (B).

(C) qPCR analyses were performed on total RNA from iHep cells in 2D cultures and iHep cells 5 days after 3D culture initiation. iHep cells were prepared from five independent experiments, designated iHep-1, iHep-2, iHep-3, iHep-4, and iHep-5.

(D) qPCR analyses were performed on total RNA from iHep cells expressing a shRNA against LacZ (sh-LacZ) or Hnf1α (sh-Hnf1α) 1 day after 3D culture initiation. sh-LacZ was used in control experiments.

(E) qPCR analyses were performed on total RNA from mock-infected iHep, iHep-5SA, and iHep-5SA/S94A cells in 2D cultures and the same cell types 5 days after 3D culture initiation.

(F) Schematic diagram of the mouse Hnf1α genomic locus and predicted Tead-binding regions (R2 and R3). Regions lacking Tead-binding sequences were used as negative controls (R1 and R4).

(G) ChIP-qPCR analyses were conducted to examine the binding of Yap and Chd4 to R1, R2, R3, and R4 in the mouse Hnf1α genomic locus using cell lysates of iHep-5SA cells 3 days after 3D culture initiation.

(H) Schematic model for upregulation of $Hnf1α$ expression and Hnf1α target gene expression in iHep cell aggregates. The Yap-Tead-Chd4 transcriptional repressor unit suppresses $Hnf1α$ expression in iHep cells. Yap inactivation in iHep cell aggregates leads to upregulation of $Hnf1α$ expression and Hnf1α target gene expression to induce hepatic maturation of iHep cells.

All data were normalized to the values for iHep cells in 2D cultures (C), iHep cells expressing sh-LacZ (D), mock-infected iHep cells in 2D cultures (E), and control experiments using an anti-immunoglobulin G (anti-IgG) antibody (Ab) (G), and the fold differences are shown. Data in (C)–(E) and (G) represent means ± SD (n = 3). *p < 0.05; **p < 0.01; n.s., not significant. See also Figures S4–S6.

EXPERIMENTAL PROCEDURES

Mice
Ten- to 12-week-old male C57BL/6 mice (Clea) and $Fah^{-/-}$ mice (Suzuki et al., 2008) were used in this study. The experiments were approved by the Kyushu University Animal Experiment Committee, and the care of the animals was in accordance with institutional guidelines.

Gene Expression Microarray and Data Analysis
Total RNA was extracted from 2D and 3D cultures of iHep cells using an RNeasy Micro Kit (QIAGEN). Microarray analyses were carried out as described previously (Sekiya and Suzuki, 2011), with kind support from Cell Innovator. Functional enrichment analyses were performed using GSEA release 2.06 and MSigDB release 2.5. Microarray data were uploaded to the GEO database (GEO: GSE106328).

Statistical Analysis
Statistical significance was analyzed by an unpaired Student's t test. Differences at $p < 0.05$ were considered statistically significant. Kaplan-Meier survival curves were statistically analyzed by the Bonferroni method using Prism software (GraphPad Prism).

SUPPLEMENTAL INFORMATION

Supplemental Information includes Supplemental Experimental Procedures and six figures and can be found with this article online at https://doi.org/10.1016/j.celrep.2018.09.010.

AUTHOR CONTRIBUTIONS

J.Y., M.U., S.M., and S.S. performed the experiments. J.Y. and A.S. analyzed and interpreted the data and wrote the paper. A.S. contributed to the conception, design, and overall project management.

DECLARATION OF INTERESTS

The authors declare no competing interests.

REFERENCES

Aragona, M., Panciera, T., Manfrin, A., Giulitti, S., Michielin, F., Elvassore, N., Dupont, S., and Piccolo, S. (2013). A mechanical checkpoint controls multicellular growth through YAP/TAZ regulation by actin-processing factors. Cell 154, 1047–1059.

Chang, T.T., and Hughes-Fulford, M. (2014). Molecular mechanisms underlying the enhanced functions of three-dimensional hepatocyte aggregates. Biomaterials 35, 2162–2171.

Desai, P.K., Tseng, H., and Souza, G.R. (2017). Assembly of hepatocyte spheroids using magnetic 3D cell culture for CYP450 inhibition/induction. Int. J. Mol. Sci. 18, 1085.

Du, Y., Wang, J., Jia, J., Song, N., Xiang, C., Xu, J., Hou, Z., Su, X., Liu, B., Jiang, T., et al. (2014). Human hepatocytes with drug metabolic function induced from fibroblasts by lineage reprogramming. Cell Stem Cell 14, 394–403.

Fan, R., Kim, N.G., and Gumbiner, B.M. (2013). Regulation of Hippo pathway by mitogenic growth factors via phosphoinositide 3-kinase and phosphoinositide-dependent kinase-1. Proc. Natl. Acad. Sci. USA 110, 2569–2574.

Gieseck, R.L., 3rd, Hannan, N.R.F., Bort, R., Hanley, N.A., Drake, R.A.L., Cameron, G.W.W., Wynn, T.A., and Vallier, L. (2014). Maturation of induced pluripotent stem cell derived hepatocytes by 3D-culture. PLoS ONE 9, e86372.

Guo, R., Xu, X., Lu, Y., and Xie, X. (2017). Physiological oxygen tension reduces hepatocyte dedifferentiation in in vitro culture. Sci. Rep. 7, 5923.

Hansen, C.G., Moroishi, T., and Guan, K.L. (2015). YAP and TAZ: a nexus for Hippo signaling and beyond. Trends Cell Biol. 25, 499–513.

Honkakoski, P., and Negishi, M. (2000). Regulation of cytochrome P450 (CYP) genes by nuclear receptors. Biochem. J. 347, 321–337.

Huang, P., He, Z., Ji, S., Sun, H., Xiang, D., Liu, C., Hu, Y., Wang, X., and Hui, L. (2011). Induction of functional hepatocyte-like cells from mouse fibroblasts by defined factors. Nature 475, 386–389.

Huang, P., Zhang, L., Gao, Y., He, Z., Yao, D., Wu, Z., Cen, J., Chen, X., Liu, C., Hu, Y., et al. (2014). Direct reprogramming of human fibroblasts to functional and expandable hepatocytes. Cell Stem Cell 14, 370–384.

Khetani, S.R., and Bhatia, S.N. (2008). Microscale culture of human liver cells for drug development. Nat. Biotechnol. 26, 120–126.

Kim, M., Kim, T., Johnson, R.L., and Lim, D.S. (2015). Transcriptional corepressor function of the hippo pathway transducers YAP and TAZ. Cell Rep. 11, 270–282.

Lee, Y.H., Sauer, B., and Gonzalez, F.J. (1998). Laron dwarfism and non-insulin-dependent diabetes mellitus in the Hnf-1α knockout mouse. Mol. Cell. Biol. 18, 3059–3068.

Lee, D.H., Park, J.O., Kim, T.S., Kim, S.K., Kim, T.H., Kim, M.C., Park, G.S., Kim, J.H., Kuninaka, S., Olson, E.N., et al. (2016). LATS-YAP/TAZ controls lineage specification by regulating TGFβ signaling and Hnf4α expression during liver development. Nat. Commun. 7, 11961.

Mauviel, A., Nallet-Staub, F., and Varelas, X. (2012). Integrating developmental signals: a Hippo in the (path)way. Oncogene 31, 1743–1756.

Miura, S., and Suzuki, A. (2014). Acquisition of lipid metabolic capability in hepatocyte-like cells directly induced from mouse fibroblasts. Front. Cell Dev. Biol. 2, 43.

Miyajima, A., Tanaka, M., and Itoh, T. (2014). Stem/progenitor cells in liver development, homeostasis, regeneration, and reprogramming. Cell Stem Cell 14, 561–574.

Ogawa, S., Surapisitchat, J., Virtanen, C., Ogawa, M., Niapour, M., Sugamori, K.S., Wang, S., Tamblyn, L., Guillemette, C., Hoffmann, E., et al. (2013). Three-dimensional culture and cAMP signaling promote the maturation of human pluripotent stem cell-derived hepatocytes. Development 140, 3285–3296.

Oshida, K., Vasani, N., Thomas, R.S., Applegate, D., Gonzalez, F.J., Aleksunes, L.M., Klaassen, C.D., and Corton, J.C. (2015). Screening a mouse liver gene expression compendium identifies modulators of the aryl hydrocarbon receptor (AhR). Toxicology 336, 99–112.

Overturf, K., Al-Dhalimy, M., Tanguay, R., Brantly, M., Ou, C.N., Finegold, M., and Grompe, M. (1996). Hepatocytes corrected by gene therapy are selected in vivo in a murine model of hereditary tyrosinaemia type I. Nat. Genet. 12, 266–273.

Sancho-Bru, P., Roelandt, P., Narain, N., Pauwelyn, K., Notelaers, T., Shimizu, T., Ott, M., and Verfaillie, C. (2011). Directed differentiation of murine-induced pluripotent stem cells to functional hepatocyte-like cells. J. Hepatol. 54, 98–107.

Sekiya, S., and Suzuki, A. (2011). Direct conversion of mouse fibroblasts to hepatocyte-like cells by defined factors. Nature *475*, 390–393.

Shih, D.Q., Bussen, M., Sehayek, E., Ananthanarayanan, M., Shneider, B.L., Suchy, F.J., Shefer, S., Bollileni, J.S., Gonzalez, F.J., Breslow, J.L., and Stoffel, M. (2001). Hepatocyte nuclear factor-1α is an essential regulator of bile acid and plasma cholesterol metabolism. Nat. Genet. *27*, 375–382.

Si-Tayeb, K., Lemaigre, F.P., and Duncan, S.A. (2010a). Organogenesis and development of the liver. Dev. Cell *18*, 175–189.

Si-Tayeb, K., Noto, F.K., Nagaoka, M., Li, J., Battle, M.A., Duris, C., North, P.E., Dalton, S., and Duncan, S.A. (2010b). Highly efficient generation of human hepatocyte-like cells from induced pluripotent stem cells. Hepatology *51*, 297–305.

Suzuki, A., Sekiya, S., Onishi, M., Oshima, N., Kiyonari, H., Nakauchi, H., and Taniguchi, H. (2008). Flow cytometric isolation and clonal identification of self-renewing bipotent hepatic progenitor cells in adult mouse liver. Hepatology *48*, 1964–1978.

Takayama, K., Kawabata, K., Nagamoto, Y., Kishimoto, K., Tashiro, K., Sakurai, F., Tachibana, M., Kanda, K., Hayakawa, T., Furue, M.K., and Mizuguchi, H. (2013). 3D spheroid culture of hESC/hiPSC-derived hepatocyte-like cells for drug toxicity testing. Biomaterials *34*, 1781–1789.

Tzanakakis, E.S., Hansen, L.K., and Hu, W.S. (2001). The role of actin filaments and microtubules in hepatocyte spheroid self-assembly. Cell Motil. Cytoskeleton *48*, 175–189.

Yimlamai, D., Christodoulou, C., Galli, G.G., Yanger, K., Pepe-Mooney, B., Gurung, B., Shrestha, K., Cahan, P., Stanger, B.Z., and Camargo, F.D. (2014). Hippo pathway activity influences liver cell fate. Cell *157*, 1324–1338.

Yimlamai, D., Fowl, B.H., and Camargo, F.D. (2015). Emerging evidence on the role of the Hippo/YAP pathway in liver physiology and cancer. J. Hepatol. *63*, 1491–1501.

Yu, F.X., Zhao, B., Panupinthu, N., Jewell, J.L., Lian, I., Wang, L.H., Zhao, J., Yuan, H., Tumaneng, K., Li, H., et al. (2012). Regulation of the Hippo-YAP pathway by G-protein-coupled receptor signaling. Cell *150*, 780–791.

Yu, F.X., Zhao, B., and Guan, K.L. (2015). Hippo pathway in organ size control, tissue homeostasis, and cancer. Cell *163*, 811–828.

Zhao, B., Wei, X., Li, W., Udan, R.S., Yang, Q., Kim, J., Xie, J., Ikenoue, T., Yu, J., Li, L., et al. (2007). Inactivation of YAP oncoprotein by the Hippo pathway is involved in cell contact inhibition and tissue growth control. Genes Dev. *21*, 2747–2761.

Zhao, B., Ye, X., Yu, J., Li, L., Li, W., Li, S., Yu, J., Lin, J.D., Wang, C.Y., Chinnaiyan, A.M., et al. (2008). TEAD mediates YAP-dependent gene induction and growth control. Genes Dev. *22*, 1962–1971.